 DOI: 10.1002/eji.201343606 Eur. J. Immunol. 2014. 44: 184–194

European Journal of Immunology

Myeloid-derived suppressor cells are key players in the resolution of inflammation during a model of acute infection

Alfredo R. Arocena[*1], *Luisina I. Onofrio*[*1], *Andrea V. Pellegrini*[1], *Antonio E. Carrera Silva*[2], *Augusto Paroli*[1], *Roxana C. Cano*[1], *Maria P. Aoki*[1] *and Susana Gea*[1]

[1] Centro de Investigación en Bioquímica Clínica e Inmunología, CIBICI-CONICET, Facultad de Ciencias Químicas, Universidad Nacional de Córdoba, Cordoba, Argentina
[2] Department of Immunobiology, School of Medicine, Yale University, New Haven, CT, USA

Myeloid-derived suppressor cells (MDSCs) are key players in the immune suppressive network. During acute infection with the causative agent of Chagas disease, *Trypanosoma cruzi*, BALB/c mice show less inflammation and better survival than C57BL/6 (B6) mice. In this comparative study, we found a higher number of MDSCs in the spleens and livers of infected BALB/c mice compared with infected B6 mice. An analysis of the two major MDSCs subsets revealed a greater number of granulocytic cells in the spleens and livers of BALB/c mice when compared with that in B6 mice. Moreover, splenic MDSCs purified from infected BALB/c mice inhibited ConA-induced splenocyte proliferation. Mechanistic studies demonstrated that ROS and nitric oxide were involved in the suppressive activity of MDSCs, with a higher number of infected $CD8^+$ T cells suffering surface-nitration compared to uninfected controls. An upregulation of NADPH oxidase p47 phox subunit and p-STAT3 occurred in MDSCs and infected IL-6 KO mice showed less recruitment of MDSCs and impaired survival. Remarkably, in vivo depletion of MDSCs led to increased production of IL-6, IFN-γ, and a Th17 response with very high parasitemia and mortality. These findings demonstrate a new facet of MDSCs as crucial regulators of inflammation during *T. cruzi* infection.

Keywords: Inflammation · MDSCs · Nitric oxide · ROS · *Trypanosoma cruzi*

Additional supporting information may be found in the online version of this article at the publisher's web-site

Introduction

Myeloid-derived suppressor cells (MDSCs) are a heterogeneous cell population consisting of immature macrophages, granulocytes, and dendritic cells as well as myeloid progenitor cells. They are considered to be one of the major components of the immune suppressive network responsible for suppressing T-cell responses in pathological conditions [1, 2] as well as in the regulation of the immune response in healthy individuals [3]. These myeloid cells are commonly identified in mice by the co-expression of the surface markers CD11b and Gr1 (Ly6G/Ly6C) and have been divided into two subsets: granulocytic (G) MDSCs with a $CD11b^+LY6G^+LY6C^{low}$ phenotype and monocytic (M) MDSCs with $CD11b^+LY6G^-LY6C^{high}$ phenotype [3, 4]. Despite their morphological similarities, G-MDSCs and neutrophils are functionally and phenotypically different. G-MDSCs, but not neutrophils, are immunosuppressive and express higher levels of arginase-1 and myeloperoxidase than neutrophils, and also have increased production of reactive oxygen species (ROS) [5, 6]. Although

Correspondence: Dr. Susana Gea
e-mail: sgea@fcq.unc.edu.ar

*These authors contributed equally to this work.

M-MDSCs and inflammatory monocytes share the same phenotype and morphology, these cells are functionally distinct since M-MDSCs are highly immunosuppressive and they express high levels of both iNOS and arginase-1. Furthermore, although iNOS expression is a hallmark of a tumoricidal/microbicidal phenotype in M1 macrophages, iNOS promotes suppressive activities in M-MDSCs. This shift in iNOS activity most likely reflects the crosstalk of iNOS with other enzymes such as NADPH oxidase to promote the production of peroxynitrites, which inhibits the proliferation and effector function of T cells [2].

MDSCs use several mechanisms in addition to the production of ROS and NO, such as triggering apoptosis of activated T cells by depleting of L-arginine, via arginase [7–10]. There is also evidence that MDSCs may suppress immune activation by inducing T regulatory cell expansion [11]. Other suppressive mechanisms that have recently been proposed include the production of TGF-β [12, 13], depletion of cysteine [8], induction of COX2 and prostaglandin E2 [1, 14–16].

Trypanosoma cruzi an obligate intracellular protozoan, is the causative agent of Chagas disease. This disease affects about 20 million people in Latin America, with 120 million persons at risk. In the past decades, mainly as a result of increased migrations, the diagnosed cases have also increased in nonendemic countries such as Canada, United States of America, and Europe. This has led to an increased risk of transmission of the infection, mainly through blood transfusion and organ transplantation [17]. Parasite persistence eventually results in severe complications in the cardiac and gastrointestinal tissues. In addition, *T. cruzi* also infects the reticuloendothelial system including the liver, spleen, and bone marrow. [18–21]. The existence of an immunosuppressive activity exerted by MDSCs during acute *T. cruzi* infection has been previously reported [22]. More recently, these authors reported the predominant induction of M-MDSCs in cardiac lesions of BALB/c mice infected with *T. cruzi* Y strain. These cells expressing iNOS/arginase-1 use suppressive mechanisms such as NO production and depletion of arginine by arginase-1 [10].

In a previous study analyzing the innate immunity induced in BALB/c and C57BL/6 (B6) mice after Tulahuen strain *T. cruzi* infection [21], we observed that B6 showed higher morbidity and mortality compared with BALB/c mice which demonstrated better tissue repair. In addition, increased and persistent levels of TNF-α, IL-6, IL-12, and IL-1β proinflammatory cytokines and very low IL-10 and TGF-β were present in the liver of B6 mice. In contrast, in BALB/c mice, the proinflammatory profile was effectively counteracted by IL-10 and TGF-β [21].

We hypothesize that B6 and BALB/c mice may exhibit differences in the mechanisms of regulation of *T. cruzi* infection induced inflammation, with MDSCs possibly playing an important role in the preservation of this homeostasis. In the present work, we focus on characterizing the major MDSCs phenotypes found during acute *T. cruzi* infection and the possible underlying suppression mechanisms occurring. Our results unequivocally demonstrate that the MDSCs induced during *T. cruzi* infection are key factors in controlling the proinflammatory immune response and consequently in determining the infection outcome.

Results

$CD11b^+Gr1^+$ cells differentially expand in liver and spleen of *T. cruzi* infected BALB/c and B6 mice

We previously observed that during *T. cruzi* infection, B6 mice developed a strong inflammatory response associated with severe liver injury whereas infected BALB/c mice showed a more balanced inflammatory response [23]. To test the hypothesis that infected B6 and BALB/c mice can exhibit differences in the mechanisms of regulation generated by MDSCs, we first studied the absolute numbers of MDSCs ($CD11b^+Gr1^+$) in intrahepatic leukocytes (IHLs) and splenocytes at 21 days postinfection (dpi). A higher number of $CD11b^+Gr1^+$ cells were detected in IHL and splenocytes from infected BALB/c compared with B6 mice (Fig. 1A). Notably, there were four times more MDSCs in BALB/c spleens compared with B6 spleens. We further observed that the number of G-MDSCs was higher in the liver and spleen of infected BALB/c mice than in B6 mice. In addition, the number of M-MDSCs was similar between both mouse strains (Fig. 1B).

Suppressor mechanism of splenic $CD11b^+Gr1^+$ cells from infected BALB/c mice

We decided to focus on the BALB/c model, in order to study the suppressor mechanisms exerted by MDSCs from this mouse breed. For this purpose, $CD11^+Gr1^+$ cells were sorted (Fig. 2A) and cultured with uninfected splenocytes in the presence of concanavalin A (Con A) or medium alone. A significant suppression of the lymphocytes proliferative response of uninfected cells was observed in the presence of MDSCs isolated from infected mice (Fig. 2B). In addition, as expected, infected splenocytes stimulated with Con A showed a potent ability to suppress the proliferative response (Fig. 2C), probably due to the suppressive effects exerted by the high rate of MDSCs present in this condition. The inhibition of ROS using a scavenger of oxygen-free radicals *N*-acetyl L-cystein (NAC) or alternatively, the inhibition of NO synthase (L-NMMA) partially blocked the MDSCs suppressive effect compared with cultures without the inhibitors (Fig. 2C). However, the arginase inhibitor (nor-NOHA) did not block suppression in this assay (data not shown). Similar results were obtained in T-cell proliferation upon anti-CD3/anti-CD28 Ab stimulation (Supporting Information Fig. 1). To investigate whether the MDSCs exerted suppression through ROS and/or NO metabolites, we added purified MDSCs from infected mice to uninfected splenocytes in the presence or absence of the specific inhibitors. A partial recovery of proliferation rates was observed in the presence of NAC and L-NMMA, suggesting that both NO and ROS were involved in the MDSCs suppressor mechanisms (Fig. 2D).

MDSCs increased ROS levels and in NADPH oxidase p47phox subunit expression

MDSCs from infected mice showed a higher fluorescent staining following PMA stimulation, compared with MDSCs from

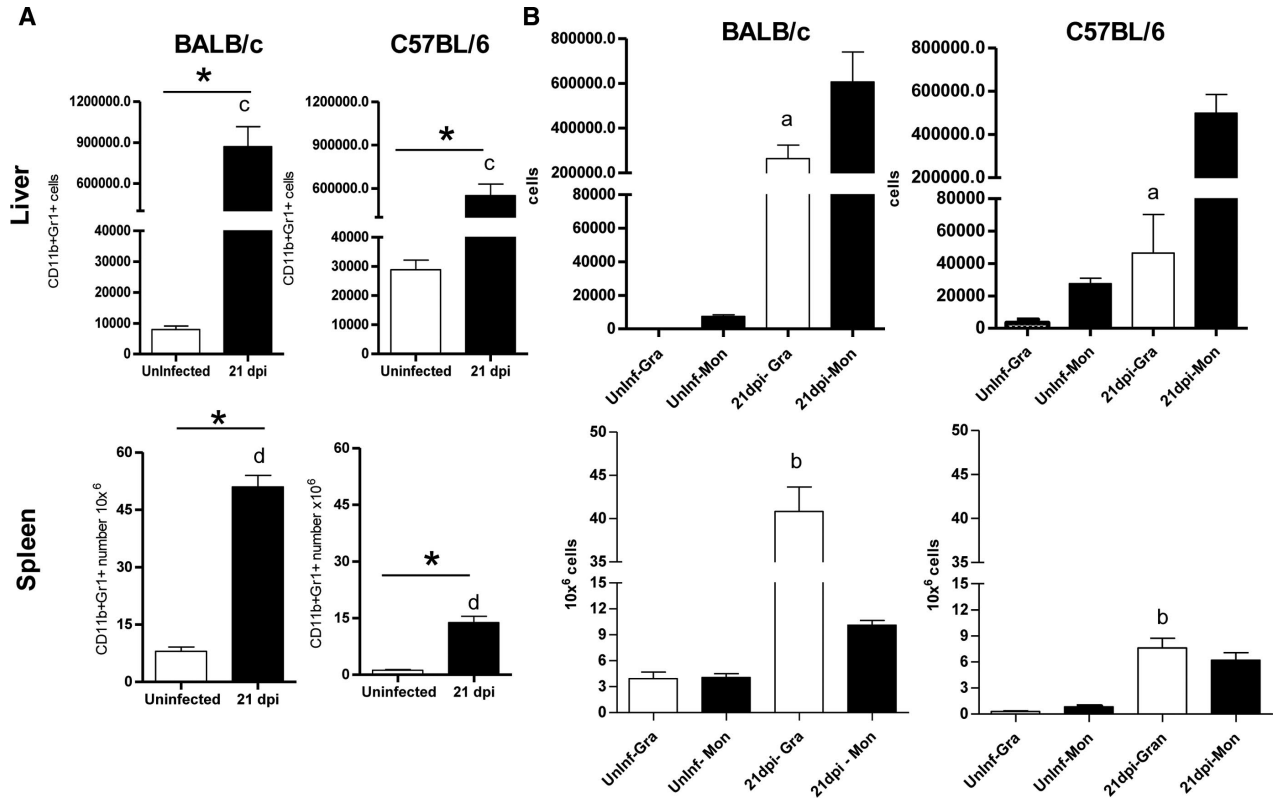

Figure 1. Gr-1$^+$CD11b$^+$ cells in liver and spleen of *Trypanosoma cruzi* infected mice. Splenocytes and intrahepatic leukocytes from infected and uninfected BALB/c and B6 mice were stained with anti-CD11b, anti-Gr-1, anti-Ly6C, and anti-Ly6G Abs. (A) The absolute numbers of Gr-1$^+$CD11b$^+$ cells in liver or spleen from infected and uninfected mice are indicated for BALB/c and B6 mice. (B) The absolute number of granulocytic CD11b$^+$Ly6G$^+$Ly6C^{low} and monocytic CD11b$^+$Ly6G-Ly6C^{high} cells in liver and spleen from infected and uninfected BALB/c and B6 mice is indicated. Data are shown as mean + SEM of three mice per group from one experiment representative of two performed. $^*p < 0.05$ versus uninfected group; a: $p < 0.05$ between strains; b: $p < 0.001$ between strains; c: $p < 0.05$ between strains; d: $p < 0.001$ between strains. p Values were calculated using t-test (A) and one-way ANOVA test (B).

uninfected mice (Fig. 3A). The NADPH oxidase complex comprises a membrane-associated low potential cytochrome b558 composed of p22^{phox} and gp91^{phox} subunits and cytosolic subunits (p47^{phox}, p40^{phox}, p67^{phox}, and Rac1 or Rac2). NADPH oxidase involves the translocation and association of cytosolic subunits with the membrane-bound cytochrome b558. [24]. Interestingly, isolated MDSCs from infected mice expressed higher levels of p47^{phox} protein than ones from uninfected mice (Fig. 3B), suggesting that the infection could induce an increase in the NADPH oxidase activity in MDSCs.

MDSCs strongly express iNOS and generate peroxynitrites

It has been previously reported that NO and peroxynitrites are crucial mediators of MDSCs-mediated suppression [3]. Therefore, we assessed the expression of iNOS in MDSCs derived from cultures of infected and uninfected splenocytes stimulated with Con A and found a threefold increase in the CD11b$^+$Gr1$^+$iNOS$^+$ cell percentage in infected compared to uninfected mice (Fig. 4A). In addition, we evaluated the tyrosine nitration on the T-cell surface. An increase in TN$^+$CD8$^+$ and TN$^+$CD4$^+$ T cells was detected in infected compared with uninfected mice (Fig. 4B). These results were corroborated by confocal imaging (Fig. 4C). Cells with these characteristics were also observed in IHL (Fig. 4B).

In addition, we tested whether splenic or hepatic MDSCs per se had the ability to produce peroxynitrites. We found that approximately 70% of infected splenic MDSCs produced this metabolite and about 58% of hepatic MDSCs had the capacity to generate peroxynitrites. In addition, almost all MDSCs from uninfected mice stained positive for intracellular nitrotyrosine (Fig. 4D).

Role of IL-6 cytokine in the expansion of MDSCs during *T. cruzi* infection

Taking into account that IL-6 is able to increase MDSCs accumulation [25], we evaluated the number of MDSCs during acute infection in IL-6 deficient mice. A significantly lower number (about threefold) of splenic MDSCs was detected in IL-6 KO compared with wild-type mice (Fig. 5A). Interestingly, IL-6 KO mice showed 100% mortality compared with the wild-type (0%) at 21 dpi (data not shown). Since MDSCs can also produce IL-6 [26], we evaluated IL-6 production at the intracellular level. A higher number of IL-6$^+$ MDSCs was observed in infected versus uninfected mice

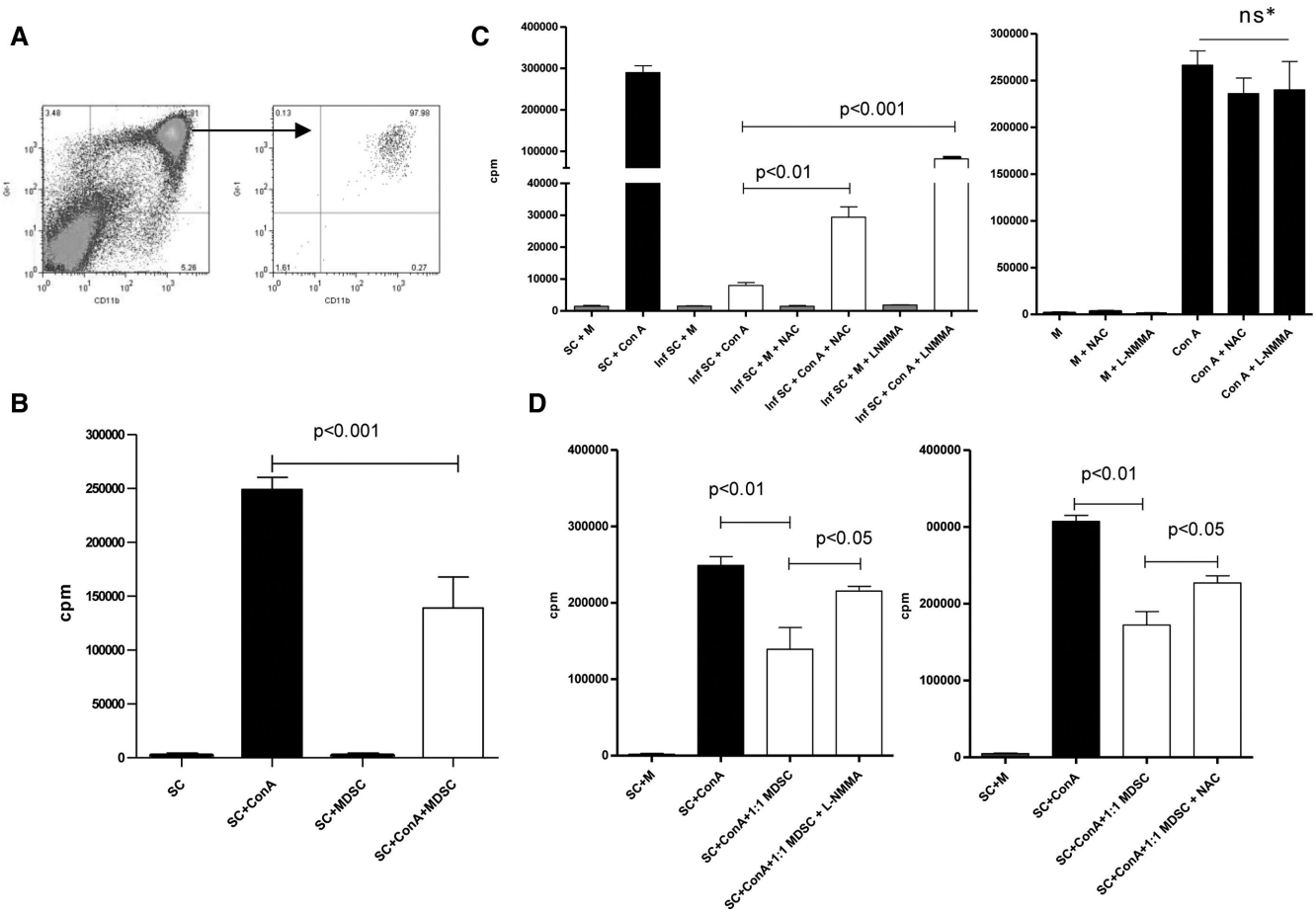

Figure 2. Suppressor mechanisms of splenic CD11b$^+$Gr1$^+$ from infected BALB/c mice. Splenocytes from infected and uninfected mice were purified, and the cells were stained with CD11b and Gr1 Abs to separate them. (A) An example of sorted MDSCs is shown. (B and C) Splenocytes from infected mice were stimulated with Con A (5 mg/mL) for 72 h and cultured (B) in the presence or absence (ratio1:1) of sorted CD11b$^+$Gr1$^+$ from infected mice, or (C) in the presence or absence of NOS inhibitor (L-NMMA) and ROS scavenger (NAC, left). As controls, splenocytes from uninfected mice were stimulated with Con A in the presence or absence of NAC and L-NMMA (right). (D) Splenocytes from uninfected mice were cultured with sorted CD11b$^+$Gr1$^+$ cells from infected mice in the presence or absence of NAC and L-NMMA. Proliferation values are represented as cpm, measured by ^{3}H-thymidine incorporation. Data are shown as mean + SEM of $n = 5$ and are from one experiment representative of two independent experiments performed. Statistical significance determined by one-way ANOVA test.

(Fig. 5B). Furthermore, high levels of IL-6 were detected in culture supernatants when splenic MDSCs were stimulated with either IL-4 (Th2 cytokine) or IFN-γ (Th1 cytokine) (Fig. 5C).

It is known that IL-6 signaling leads to the phosphorylation of the signal transducer and activator of transcription-3 (STAT3) transcription factor, which plays a critical role in the accumulation of MDSCs [2, 27]. Accordingly, we observed p-STAT3 in 70% of infected splenic MDSCs versus 45% in uninfected cells (Fig. 5D). This finding was supported by confocal microscopy studies (Fig. 5E).

Effect of in vivo reduction of MDSCs by 5-fluorouracil (5FU) treatment during *T. cruzi* infection

To evaluate the importance of MDSCs during parasite infection in BALB/c mice, the drug 5-fluorouracil (5FU) was used at 10 and/or 15 dpi. As has been previously demonstrated, 5FU 50 mg/kg selectively induces splenic MDSCs apoptotic cell death in vitro and in vivo, whereas it has no significant effect on T cells, NK, dendritic, or B cells [28]. Using the 5FU reported dose, a reduction of CD11b$^+$Gr1$^+$ was observed for both treatments with it being highly significant at 15 dpi (Fig. 6A). Moreover, 5FU treatment effectively reduced both G- and M-MDSCs subpopulations in a similar manner (Supporting Information Fig. 2) while not altering the frequency of the other cell populations (Supporting Information Fig. 3).

With the purpose of analyzing the relevance of MDSCs as key factors for maintaining homeostasis, we analyzed at 21 dpi the parasitemia and survival of treated mice after a dose of 5FU at 10 or 15 dpi, or two doses, at 10 plus 15 dpi, and the results were compared with those of untreated controls. Surprisingly, when 5FU was administered at 10 dpi, the parasitemias were lower compared with those of untreated controls, whereas the parasitemias were significantly higher when the drug was given at 15 dpi (Fig. 6B). In addition, mouse survival was about 50% when

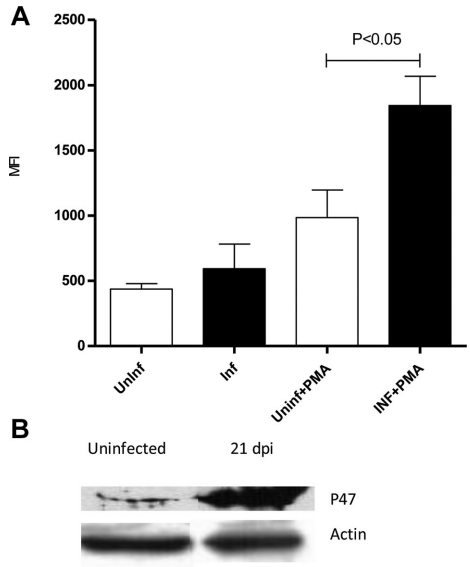

Figure 3. Increased ROS levels and upregulation of NADPH oxidase p47 ^{phox} subunit were detected in splenic MDSCs from infected BALB/c mice. (A) Spleens from infected and uninfected mice were collected at 21 dpi. Splenocytes were stimulated with PMA and labeled with anti-Gr1 and anti-CD11b Abs. ROS were measured in Gr-1$^+$CD11b$^+$ cells by labeling cells with the oxidation-sensitive dye H_2DCFDA as described in the Materials and methods. The mean fluorescence intensity (MFI) is shown as mean + SEM of four mice per group from one experiment representative of two performed. Statistical significance determined by one-way ANOVA test. (B) P47phox was analyzed by Western blot in sorted Gr-1$^+$CD11b$^+$ cell lysates derived from splenocytes from infected and uninfected mice. β-actin was used as a loading control. Data shown are representative of two experiments each performed with three mice.

5FU was administered at 10 dpi whereas the survival was approximately 20% in mice treated at 15 dpi, but there was no survival when two doses were administered, 10 plus 15 dpi (Fig. 6C).

In parallel, we also analyzed whether MDSCs depletion at 15 dpi was able to restore the Con A proliferative response of infected splenocytes. As expected, a recovery of the splenocytes proliferation was observed (Fig. 7A). Consistent with this result, a significant reduction in the percentage of CD8$^+$TN$^+$ T cells (Fig. 7B) was associated with an increase in the percentage of activated CD107a$^+$CD8$^+$ T cell (Fig. 7C). CD107a has been previously shown to be a marker for cytotoxic CD8$^+$ T-cell activity [29]. Interestingly, we also detected a higher level of IL-6 and IFN-γ inflammatory cytokines in plasma from 5FU-treated mice compared with untreated ones, as well as an elevated concentration of TNF-α in both untreated and treated groups (Fig. 7D).

Finally, the 5FU treatment increased the number of Th1 (CD4$^+$IFN-γ$^+$) and Th17 (CD4$^+$IL-17A$^+$) cells (Fig. 7E) at 19 dpi.

Discussion

It is clear that there is a complex interplay between host and parasite that influences the outcome of an infection. Recently, we demonstrated that during acute *T. cruzi* infection, BALB/c mice showed a reduced inflammatory response, and an improved survival and tissue repair compared with B6 mice, the latter developed a severe inflammation and liver/cardiac pathology [23]. In the present study, our data clearly indicate that there was a higher number of MDSCs infiltrating the liver and spleen of infected BALB/c mice than in B6 mice. An analysis of MDSCs subsets in the liver and spleen revealed that the number of G-MDSCs was higher in infected BALB/c with respect to B6 mice, suggesting a protective role for G-MDSCs in the resolution of inflammation. In agreement with this concept, an increased accumulation of G-MDSCs has been correlated with reduced tissue injury in various experimental models of inflammation [30–32]. In cancer, the frequency of each MDSCs subset appears to be influenced by the type of tumor [2].

The study of the suppressor mechanisms exerted by splenic MDSCs from infected BALB/c mice revealed that the suppression of lymphocyte proliferative response was mediated by ROS and NO production but not by arginase activity. A suppressive mechanism mediated by NO during *T. cruzi* infection has previously been reported [22]. When MDSCs were isolated and added to the cultures, the suppressive activity was partial, suggesting that other cells, likely regulatory T cells, might be also exerting the suppressive activity during the acute infection [33].

Taking into account that mature macrophages (F4/80$^+$) produce elevated levels of NO and that M-MDSCs may express F4/80 marker [34,35], our results revealed that about 20% of MDSCs co-express F4/80 (data not shown). In addition, a cross-talk between MDSCs and macrophages subverts type 1 toward type 2 immunity [36]. Related to this, we previously observed a mixed Th1/Th2 profile in the BALB/c mice versus Th1 dominant response in B6 mice during parasitic infection [23, 37]. Our results indicate that infection with the Tulahuen strain of *T. cruzi* induced the recruitment of MDSCs subsets with different phenotypes. On the other hand, it has been demonstrated that cardiac M-MDSCs suppression is mainly mediated by NO and Arginase-1 during Y strain *T. cruzi* infection [10]. Thus, MDSCs tissue localization, parasite strain, tropism, and virulence could be important factors for their better characterization.

Various interesting studies have demonstrated that G-MDSCs may suppress CD8$^+$ T cells by producing ROS that are triggered by an increased activation of STAT3 and NADPH oxidase [3, 27]. In agreement with this evidence, our results revealed an upregulation of NADPH oxidase and p-STAT3 in splenic MDSCs from infected BALB/c mice. In fact STAT3 not only prevents apoptosis but is also a crucial regulator of MDSCs expansion [38–40].

Many of the biological effects attributed to NO are actually mediated by peroxynitrites that are crucial mediators of MDSCs-mediated suppression. These peroxynitrites induce the nitration of amino acids such as tyrosine, among others, and cause several alterations in T cells including the loss of TCR ζ–chain expression [2]. Our results have shown that the percentage of splenic CD8$^+$ T cells, which were nitrotyrosine positive, was substantially higher in infected BALB/c mice than in uninfected ones. Related to this, the nitration of tyrosine within the TCR/CD8 complex induced by MDSCs during cell–cell contact has been previously demonstrated in a tumor model [41].

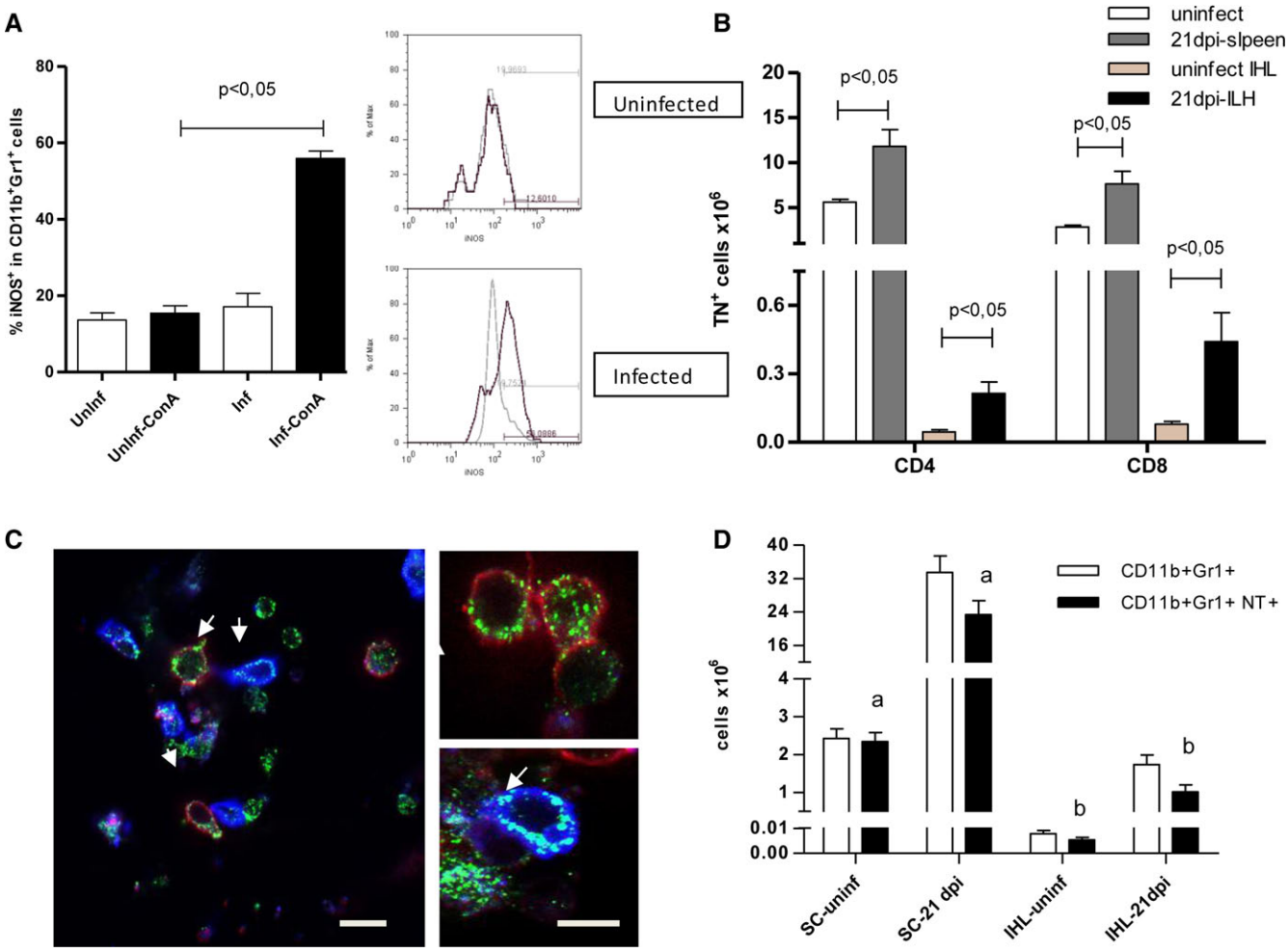

Figure 4. iNOS expression and peroxynitrite production by $CD11b^+Gr1^+$ from BALB/c mice. (A) Splenocytes from infected or uninfected mice were stimulated with Con A (5 mg/mL) for 48 h. Spleen cells were then stained with anti-Gr-1, anti-CD11b, and anti-iNOS Abs. The percentage of iNOS in $Gr\text{-}1^+$ $CD11b^+$ MDSCs was measured by flow cytometry and shown as mean + SEM of three mice from one experiment representative of two performed. Statistical significance determined by one-way ANOVA test. (B) Expression of tyrosine nitration in $CD4^+$ and $CD8^+$ T cells. Splenocytes and IHLs from infected and uninfected mice were stained with anti-CD4, anti-CD8, and anti- TN Abs. The absolute numbers of $CD4^+$ TN^+ cells and $CD8^+$ TN^+ cells under different conditions are shown as mean + SEM of four mice from one experiment representative of two performed. Statistical significance determined by two-way ANOVA test. (C) Splenocytes from infected mice were cultured with Con A for 48 h. The cells were labeled with anti-CD4-allophycocyanin (blue), anti-CD8-PE (red) and anti- TN -Alexa 488 (green), and visualized using confocal microscopy. Scale bar = 10 μm. Arrows denote positive staining for TN localization. (D) The absolute numbers of spleen and IHL MDSCs from infected and uninfected mice expressing intracellular nitrotyrosine are shown. Cells were stained with anti-Gr-1, anti-CD11b, and intracellular nitrotyrosine Abs. Expression of nitrotyrosine was evaluated in the $CD11b^+Gr1^+$gate. The total numbers of $CD11b^+Gr1^+$ (white bars) and $CD11b^+Gr1^+$ TN^+ (black bars) are shown as mean + SEM of four mice from one experiment representative of two performed. **a** and **b,** $p < 0.05$ versus uninfected group, two-way ANOVA test.

In agreement with the inhibition of IL-6 abrogating the accumulation of MDSCs in tumor-bearing mice [42], our data revealed a significant reduction of splenic MDSCs in IL-6KO versus wild-type mice, associated with a 100% mortality, thus suggesting the significance of IL-6 in the recruitment of MDSCs in order to maintain homeostasis during infection.

The relevance of MDSCs in our model was evaluated by reduction assays using 5FU treatment. After treatment, a diminution of TN on $CD8^+$ T cells was associated with elevated $CD8^+$ cell activation, as measured by CD107a expression. In addition, IL-6 and IFN-γ were dramatically increased in plasma compared with untreated mice. This result shows that the lack of MDSCs during *T. cruzi* infection also generated alterations at the systemic level, which could partially explain why these mice did not survive as well as the controls. We speculate that the excessive T-cell activation may potentiate the mechanism of activation-induced cell death leading to elimination of parasite-specific T lymphocytes [43]. An excessive inflammation worsens the disease and probably compromises the host's ability to eradicate infection [44]. Indeed, in our study, the MDSCs depletion led to the highest parasitemia. Conversely, MDSCs depletion in tumor models has been shown to enhance the therapeutic vaccination responses, leading to tumor cell death [45]. Although clinical research is currently in progress to suppress MDSCs in cancer in order to improve antineoplasic treatments, such approaches may not be beneficial in infectious diseases [46].

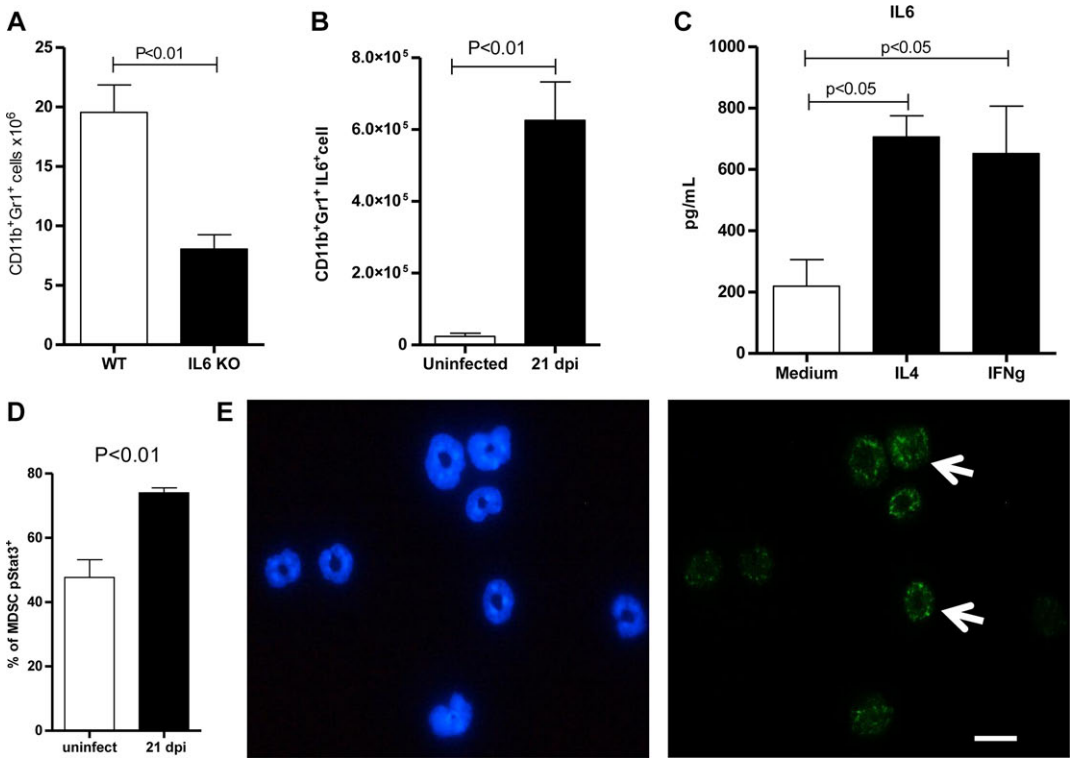

Figure 5. Rol of IL-6 in the expansion of MDSCs during *Trypanosoma cruzi* infection. (A) Splenocytes from infected B6 and IL-6 KO mice were stained with anti-CD11b and anti-Gr-1 Abs at 17 dpi. The absolute number of Gr-1$^+$CD11b$^+$ cells is shown. (B) Splenic Gr-1$^+$CD11b$^+$ cells from infected and uninfected BALB/c mice were examined for IL-6 expression by intracellular staining using flow cytometry after stimulation with PMA plus ionomycin in the presence of monensin. (C) Sorted MDSCs were cultured for 24 h in the presence or absence of 100 ng/mL IL-4 or IFN-γ, and the levels of IL-6 were examined by ELISA. (D) Sorted MDSCs from infected and uninfected mice were cultured for 24 h and stimulated with ConA. MDSCs were then intracellularly stained for p-STAT3. (A–D) Data are shown as mean + SEM of three to five mice per group from one experiment representative of two performed. Statistical significance determined by *t*-test. (E) Freshly isolated spleen cells of infected BALB/c mice were stained with mAb against CD11b and Gr-1, and sorted; cytospin preparations were stained with Hoescht (blue) and p-STAT3 (green). Arrows denote positive staining for p-STAT3 localization. Images are representative of two independent experiments with similar results. Scale bar: 10 μm.

Finally, we found a negative relationship between the number of MDSCs and Th1/Th17 cells in the spleens of infected BALB/c mice. In agreement with this, a negative correlation between circulating MDSCs and Th17 cells was previously found in rheumatoid arthritis patients [47]. These new findings provide unique insights into the pleiotropic functions of MDSCs and may help to explain how these cells control Th1/Th17 responses under these pathological conditions.

Summing up, our data have identified a new facet of MDSCs as beneficial players in reducing parasite replication, enhancing the resolution of the infection, and preventing the excessive host's inflammation.

Materials and methods

Mice, infection, parasitemia, and MDSCs in vivo depletion

BALB/c and B6 mice were purchased from National University of La Plata, Bs As, Argentina and B6 IL-6-knockout (IL-6KO) mice were obtained from the Jackson Laboratory, Bar Harbor, ME, USA. Animals were maintained at the Animal Resource Facility of the CIBICI-CONICET (NIH-USA assurance number A5802–01) following the recommendations in the Guide for the Care and Use of Experimental Animals (Canadian Council on Animal Care) and approved by the CIBICI-CONICET. Groups of mice (6–8 weeks old) were infected by i.p. injection with 10^3 blood trypomastigotes Tulahuén strain. Parasitemia was measured as previously described [23]. Noninfected mice of each strain were used as controls. Parasites were maintained by serial passages from mouse to mouse.

For MDSCs in vivo depletion treatments, BALB/c mice received a single or double i.p. injection of 5FU (50 mg/kg). Mice injected with PBS were used as untreated controls.

Isolation of mouse cells

Spleen and liver cells were obtained and homogenized through a tissue strainer. IHL were obtained after 20 min centrifugation (600 $\times$ *g*) in a 35 and 70% bilayer Percoll (Sigma) gradient. Viable cell numbers were determined by Trypan blue exclusion. Splenic MDSCs were isolated by FACS Aria cell sorter using staining with PE-anti-Gr-1 and APC-anti-CD11b Abs (BD Pharmingen), with a purification of approximately 98%.

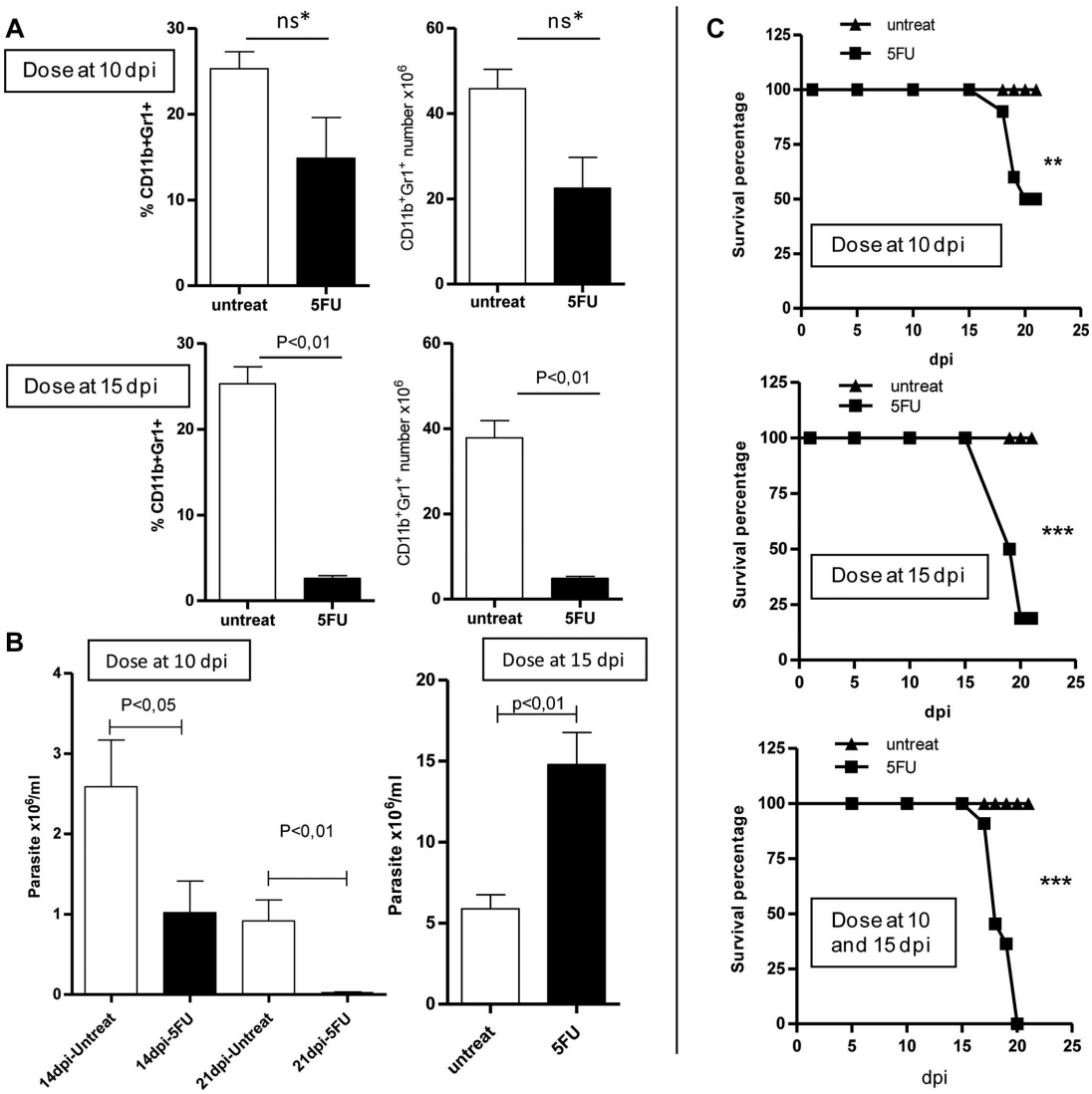

Figure 6. Effect of 5FU treatment during *Trypanosoma cruzi* infection. Infected BALB/c mice were treated or not with 5FU (50 mg/kg) at 10 dpi, at 15 dpi, or at 10 and 15 dpi. (A) Splenocytes from different groups were stained with anti-CD11b and anti-Gr-1 Abs. The percentage and the absolute number of spleen Gr-1$^+$CD11b$^+$ cells are shown. (B) The parasite number per milliliter was measured in the blood. When 5FU was given at 10 dpi, the analyses were performed at 14 and 21 dpi, and when the treatment was carried out at 15 dpi, the analysis was performed at 19 dpi. (A and B) Data are shown as mean + SEM of six to eight mice per group from one experiment representative of two performed. Statistical significance determined by one-way ANOVA and *t*-test. (C) The survival percentage at 21 dpi was analyzed for the three groups. Data are shown for a single experiment representative of two performed. $^{**}p < 0.01$ and $^{***}p < 0.001$ versus untreated group, Gehan-Breslow-Wilcoxon test.

Lymphoproliferation assays

Spleen cells (splenocytes) were cultured in RPMI 1640 medium supplemented with 2 mM glutamine, 50 mM 2-ME, and 40 mg/mL gentamicin containing 10% FBS in triplicate in flat-bottomed 96-well plates at 2×10^5 cells/well (200 μL/well). After incubating at 37°C and 5% CO_2 for 48 h, 1 μCi ^{3}H-thymidine (Amersham) was added to each well. The cultures were harvested 18 h later and then processed for measurement of incorporated radioactivity in a liquid scintillation counter. The inhibitors of NO, 200 uM L-NMMA; arginase, 40 uM nor-NOHA (N^W-hydroxyl-nor-L-arginine) (Calbiochem); or ROS scavenger, 5 mM NAC (*N*-acetyl L-cystein) (Sigma) were added at the beginning of the culture.

Flow cytometry

One million of SCs or IHLs were incubated in 1% FBS 1% BSA in PBS with the relevant Abs. Intracellular cytokine staining [48], nitrotyrosine staining [35], and detection of CD107a (BioLegend) [49] were made as previously described. For iNOS detection, splenocytes were cultured and stimulated with Con A (5 mg/mL) for 48 h. Then, cells were stained with allophycocyanin-anti-CD11b (clone M170) and PE-anti-Gr1, fixed, permeabilized with Cytofix/Cytoperm buffer, and were incubated with rabbit polyclonal anti-iNOS Ab (BD Bioscience). After washing, samples were examined using BD FACS Canto II flow cytometer (BD Biosciences).

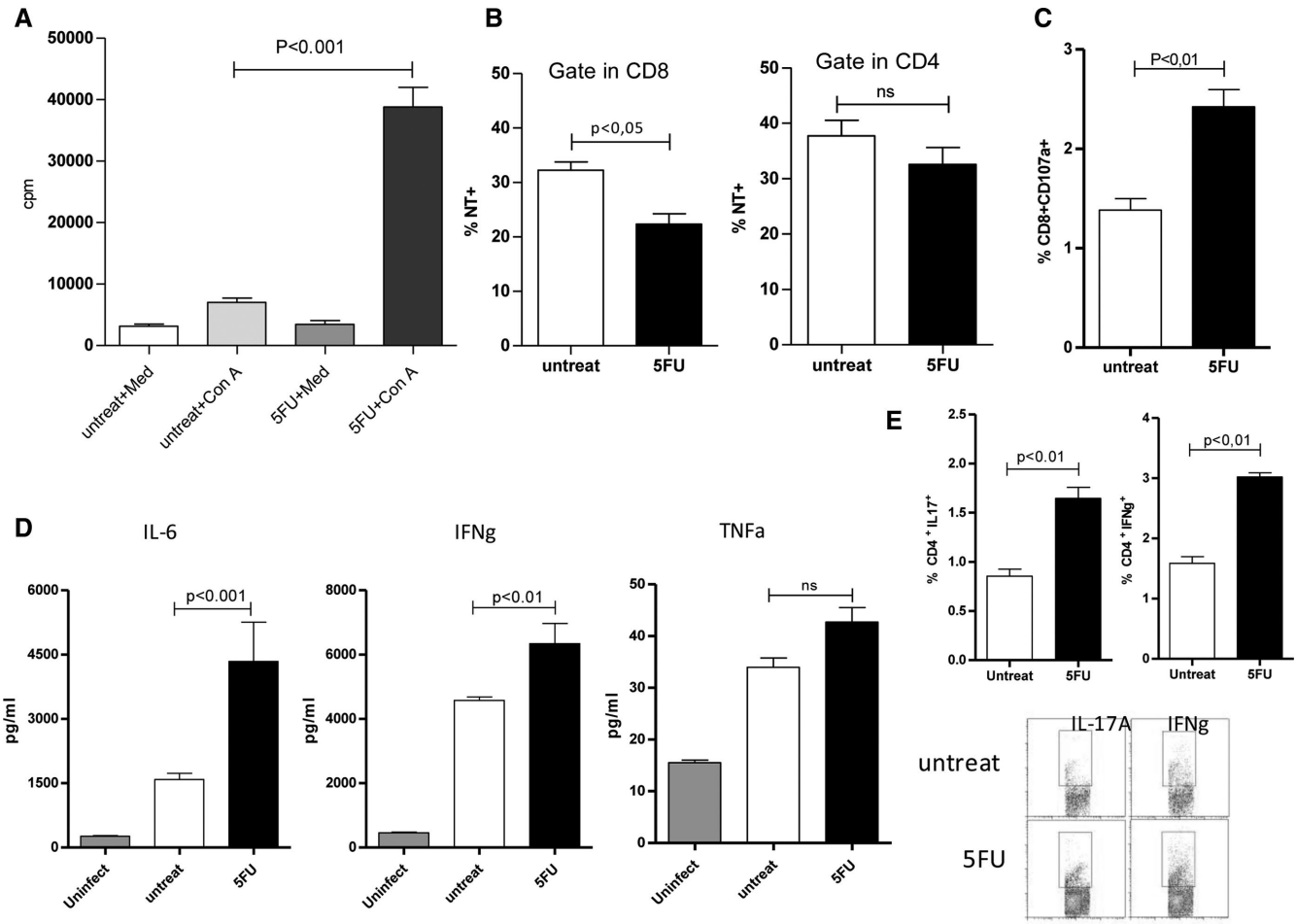

Figure 7. Different immune consequences in *Trypanosoma cruzi*-infected BALB/c mice treated with 5FU. (A) Recovery of ConA proliferative response. Splenocytes from infected BALB/c mice treated or not with 5FU were stimulated with Con A (5 mg/mL) for 72 h. Proliferation values are represented as ^{3}H-thymidine incorporation. Each experiment was performed in triplicate. (B) Percentages of tyrosine nitration on $CD8^+$ and $CD4^+$ T cells under different conditions. Splenocytes of 5FU treated and untreated mice were stained with anti-CD4, anti-CD8, and anti-TN Abs. (C) Effect of MDSCs depletion on the number of $CD107a^+CD8^+$ T cells. Splenocytes from both groups were cultured in the presence of PMA plus ionomycin and monensin for 5 h and stained with antibodies against CD107a and CD8. (D) IL-6, IFN-γ, and TNF-α levels were measured in plasma by ELISA. (E) Splenocytes from infected mice treated or not with 5FU were purified and examined for $CD4^+$ T cells IL-17A or IFN-γ expression by intracellular staining using flow cytometry after stimulation with PMA plus ionomycin in the presence of monensin. All data are shown as mean + SEM of three to five mice per group from one experiment representative of two performed. Statistical significance determined by one-way ANOVA and *t*-test.

The Abs conjugated were allophycocyanin-anti-Ly6G/Ly6C (Gr-1, clone RB6–8C5), PE-anti-Ly6G (clone 1A8), FITC-anti-Ly6C (clone AL-21) (BD Bioscience), allophycocyanin-anti-CD4 (clone GK1.5)(BioLegend), PE-anti-CD8 (clone 53-6.7), PE-anti-IL6 (MP5-20F3), PE-anti-IFNγ (XMG1.2,), PE-anti-IL-17A (clone eBio17B7) (eBioscience), and anti-Phospho-Stat3 (Tyr705)(clone D3A7) (Cell Signaling).

Oxidation-sensitive dye DCFDA (Molecular Probes/Invitrogen), was used to measure ROS production [27].

Measurement of cytokines

Cytokine levels were determined by ELISA sandwich for detecting TNF-α, IL6, and IFN-γ (eBioscience) in plasma and in culture supernatants from sorted MDSCs cultured in supplemented RPMI 1640 at 24 h.

Fluorescence microscopy

Splenocytes were cultured with ConA for 48 h, fixed in 4% paraformaldehyde, blocked with PBS-BSA 1% and labeled with allophycocyanin-anti-CD4, PE-anti-CD8, and Alexa Fluor 488-anti-NT and visualized using FV1000 (Olympus) confocal microscope. Sorted $CD11b^+Gr1^+$ were put on a slide by the citospin technique and were stained with DNA-binding fluorochrome Hoechst 33 258 (2 ug/mL) and FITC-anti-phosphoSTAT3. Slides were observed with a NIKON ECLIPE Microscope.

Western blot

Purified MDSCs were washed and lysed (1% Triton X-100, 0.5% sodium deoxicholate, 9% SDS, 1 mM sodium ortovanadate, and

10 g PMSF in PBS). Aliquots of tissue lysates, were separated on a 10% SDS-PAGE and transferred to nitrocellulose membranes. After blocking, they were incubated with rabbit polyclonal Ab anti-p47phox (Santa Cruz) followed by HRP-anti-rabbit Ab (Sigma) and assayed using the ECL chemiluminescent system. Protein loading was visualized by anti-actin Ab (Santa Cruz).

Statistical analysis

Experimental differences over the controls were analyzed with the Student's *t*-test and nonparametric test and differences with *p*-value of <0.05 were considered to be significant. Graph Pad Prism version 5.00 for Windows (GraphPad Software, USA) was employed. Welch correction was applied when different variances were observed. All experiments were repeated at least two times to test the reproducibility of results.

Acknowledgements: S.G. and M.P.A. are Research Career Investigator from CONICET. A.A, L.I.O., A.P., A.E.C.S, A.P., and R.C.C. thank CONICET and SECYT for the fellowships granted. We thank Alejandra Romero, Pilar Crespo, Paula Abadie, and Fabricio Navarro for their skillful technical assistance and would like to thank Dr. Paul Hobson, native speaker, for revision of the manuscript. This work was supported with grants from Agencia Nacional de Promoción Científica y Tecnológica (ANPCYT), Consejo Nacional de Investigaciones Científicas y Técnicas (CONICET) Argentina, and Secretaría de Ciencia y Tecnología de la Universidad Nacional de Córdoba (SECYT-UNC).

Conflict of interest: The authors declare no financial or commercial conflict of interest.

References

1 **Talmadge, J. E.**, Pathways mediating the expansion and immunosuppressive activity of myeloid-derived suppressor cells and their relevance to cancer therapy. *Clin. Cancer Res.* 2007. **13**: 5243–5248.

2 **Gabrilovich, D. I., Ostrand-Rosenberg, S. and Bronte, V.**, Coordinated regulation of myeloid cells by tumours. *Nat. Rev. Immunol.* 2012. **12**: 253–268.

3 **Gabrilovich, D. I. and Nagaraj, S.**, Myeloid-derived suppressor cells as regulators of the immune system. *Nat. Rev. Immunol.* 2009. **9**: 162–174.

4 **Movahedi, K., Guilliams, M., Van den Bossche, J., Van den Bergh, R., Gysemans, C., Beschin, A., De Baetselier, P. et al.**, Identification of discrete tumor-induced myeloid-derived suppressor cell subpopulations with distinct T cell-suppressive activity. *Blood* 2008. **111**: 4233–4244.

5 **Youn, J. I., Collazo, M., Shalova, I. N., Biswas, S. K. and Gabrilovich, D. I.**, Characterization of the nature of granulocytic myeloid-derived suppressor cells in tumor-bearing mice. *J. Leukoc. Biol.* 2012. **91**: 167–181.

6 **Brandau, S., Trellakis, S., Bruderek, K., Schmaltz, D., Steller, G., Elian, M., Suttmann, H. et al.**, Myeloid-derived suppressor cells in the peripheral blood of cancer patients contain a subset of immature neutrophils with impaired migratory properties. *J. Leukoc. Biol.* 2011. **89**: 311–317.

7 **Ostrand-Rosenberg, S. and Sinha, P.**, Myeloid-derived suppressor cells: linking inflammation and cancer. *J. Immunol.* 2009. **182**: 4499–4506.

8 **Srivastava, M. K., Sinha, P., Clements, V. K., Rodriguez, P. and Ostrand-Rosenberg, S.**, Myeloid-derived suppressor cells inhibit T-cell activation by depleting cystine and cysteine. *Cancer Res.* 2010. **70**: 68–77.

9 **Apolloni, E., Bronte, V., Mazzoni, A., Serafini, P., Cabrelle, A., Segal, D. M., Young, H. A. et al.**, Immortalized myeloid suppressor cells trigger apoptosis in antigen-activated T lymphocytes. *J. Immunol.* 2000. **165**: 6723–6730.

10 **Cuervo, H., Guerrero, N. A., Carbajosa, S., Beschin, A., De Baetselier, P., Girones, Fresno, M.**, Myeloid-derived suppressor cells infiltrate the heart in acute *Trypanosoma cruzi* infection. *J. Immunol.* 2011. **187**: 2656–2665.

11 **Huang, B., Pan, P. Y., Li, Q., Sato, A. I., Levy, D. E., Bromberg, J., Divino, C.M. et al.**, Gr-1+CD115+ immature myeloid suppressor cells mediate the development of tumor-induced T regulatory cells and T-cell anergy in tumor-bearing host. *Cancer Res.* 2006. **66**: 1123–1131.

12 **Li, H., Han, Y., Guo, Q., Zhang, M. and Cao, X.**, Cancer-expanded myeloid-derived suppressor cells induce anergy of NK cells through membrane-bound TGF-beta 1. *J. Immunol.* 2009. **182**: 240–249.

13 **Yang, L., Huang, J., Ren, X., Gorska, A. E., Chytil, A., Aakre, M., Carbone, D. P. et al.**, Abrogation of TGF beta signaling in mammary carcinomas recruits Gr-1+CD11b+ myeloid cells that promote metastasis. *Cancer Cell* 2008. **13**: 23–35.

14 **Rodriguez, P. C., Hernandez, C. P., Quiceno, D., Dubinett, S. M., Zabaleta, J., Ochoa, J. B., Gilbert, J. et al.**, Arginase I in myeloid suppressor cells is induced by COX-2 in lung carcinoma. *J. Exp. Med.* 2005. **202**: 931–939.

15 **Marigo, I., Dolcetti, L., Serafini, P., Zanovello, P. and Bronte, V.**, Tumor-induced tolerance and immune suppression by myeloid derived suppressor cells. *Immunol. Rev.* 2008. **222**: 162–179.

16 **Ostrand-Rosenberg, S.**, Myeloid-derived suppressor cells: more mechanisms for inhibiting antitumor immunity. *Cancer Immunol. Immunother.* 2010. **59**: 1593–1600.

17 **Schmunis, G. A. and Yadon, Z. E.**, Chagas disease: a Latin American health problem becoming a world health problem. *Acta Trop.* 2010. **115**: 14–21.

18 **Bouzahzah, B., Nagajyothi, F., Desruisseaux, M. S., Krishnamachary, Factor, S. M., Cohen, A. W., Lisanti, M. P. et al.**, Cell cycle regulatory proteins in the liver in murine *Trypanosoma cruzi* infection. *Cell Cycle* 2006. **5**: 2396–2400.

19 **Sardinha, L. R., Elias, R. M., Mosca, T., Bastos, K. R., Marinho, C. R., D'Império Lima, M. R., Alvarez, J. M.**, Contribution of NK, NK T, gamma delta T, and alpha beta T cells to the gamma interferon response required for liver protection against *Trypanosoma cruzi*. *Infect. Immun.* 2006. **74**: 2031–2042.

20 **Ronco, M. T., Frances, D. E., Ingaramo, P. I., Quiroga, A. D., Alvarez, M. L., Pisani G. B., Revelli, S. S. et al.**, Tumor necrosis factor alpha induced by *Trypanosoma cruzi* infection mediates inflammation and cell death in the liver of infected mice. *Cytokine* 2010. **49**: 64–72.

21 **Carrera-Silva, E. A., Guinazu, N., Pellegrini, A., Cano, R. C., Arocena, A., Aoki, M. P., Gea, S.**, Importance of TLR2 on hepatic immune and non-immune cells to attenuate the strong inflammatory liver response during *Trypanosoma cruzi* acute infection. *PLoS Negl. Trop. Dis.* 2010. **4**: e863.

22 **Goni, O., Alcaide, P. and Fresno, M.**, Immunosuppression during acute *Trypanosoma cruzi* infection: involvement of Ly6G (Gr1(+))CD11b(+)immature myeloid suppressor cells. *Int. Immunol.* 2002. **14**: 1125–1134.

23 **Carrera-Silva, E. A., Cano, R. C., Guinazu, N., Aoki, M. P., Pellegrini, A. and Gea, S.**, TLR2, TLR4 and TLR9 are differentially modulated in liver lethally injured from BALB/c and C57BL/6 mice during *Trypanosoma cruzi* acute infection. *Mol. Immunol.* 2008. **45**: 3580–3588.

24 **Dworakowski, R., Anilkumar, N., Zhang, M. and Shah, A. M.**, Redox signalling involving NADPH oxidase-derived reactive oxygen species. *Biochem. Soc. Trans.* 2006. **34**: 960–964.

25 **Cheng, L., Wang, J., Li, X., Xing, Q., Du, P., Su, L. and Wang, S.**, Interleukin-6 induces Gr-1+CD11b +myeloid cells to suppress CD8+ T cell-mediated liver injury in mice. *PLoS One* 2011. **6**: e17631.

26 **Chalmin, F., Ladoire, S., Mignot, G., Vincent, J., Bruchard, M., Remy-Martin, J. P., Boireau, W. et al.**, Membrane-associated Hsp72 from tumor-derived exosomes mediates STAT3-dependent immunosuppressive function of mouse and human myeloid-derived suppressor cells. *J. Clin. Invest.* 2010. **120**: 457–471.

27 **Corzo, C. A., Cotter, M. J., Cheng, P., Cheng, F., Kusmartsev, Sotomayor, E., Padhya, T. et al.**, Mechanism regulating reactive oxygen species in tumor-induced myeloid-derived suppressor cells. *J. Immunol.* 2009. **182**: 5693–5701.

28 **Vincent, J., Mignot, G., Chalmin, F., Ladoire, S., Bruchard, M., Chevriaux, A., Martin, F. et al.**, 5-Fluorouracil selectively kills tumor-associated myeloid-derived suppressor cells resulting in enhanced T cell-dependent antitumor immunity. *Cancer Res.* 2010. **70**: 3052–3061.

29 **Betts, M. R., Brenchley, J. M., Price, D. A., De Rosa, S. C., Douek, Roederer, M., Koup, R. A.**, Sensitive and viable identification of antigen-specific CD8+ T cells by a flow cytometric assay for degranulation. *J. Immunol. Methods* 2003. **281**: 65–78.

30 **Mishra, P. K., Morris, E. G., Garcia, J. A., Cardona, A. A. and Teale, J. M.**, Increased accumulation of regulatory granulocytic myeloid cells in mannose receptor C type 1 deficient mice correlates with protection in mouse model of NCC. *Infect. Immun.* 2013. **81**: 1052–1063.

31 **Ioannou, M., Alissafi, T., Lazaridis, I., Deraos, G., Matsoukas, Gravanis, A., Mastorodemos, V.**, Crucial role of granulocytic myeloid-derived suppressor cells in the regulation of central nervous system autoimmune disease. *J. Immunol.* 2012. **188**: 1136–1146.

32 **Su, H., Cong, X. and Liu, Y. L.**, Transplantation of granulocytic myeloid derived suppressor cells (G-MDSCs) could reduce colitis in experimental murine models. *J. Dig. Dis.* 2013. **14**: 251–258.

33 **Knubel, C. P., Martinez, F. F., Acosta Rodriguez, E. V., Altamirano, A., Rivarola, H. W., Diaz Luján, C., Fretes, R. E. et al.**, 3-Hydroxy kynurenine treatment controls T. cruzi replication and the inflammatory pathology preventing the clinical symptoms of chronic Chagas disease. *PLoS One* 2011. **6**: e26550.

34 **Andrade, D., Serra, R., Svensjö, E., Lima, A. P., Ramos, E. S. J., Fortes, F. S., Morandini, A.C. et al.**, *Trypanosoma cruzi* invades host cells through the activation of endothelin and bradykinin receptors: a converging pathway leading to chagasic vasculopathy. *Br. J. Pharmacol.* 2012 **165**: 1333–1347.

35 **Youn, J. I., Nagaraj, S., Collazo, M. and Gabrilovich, D. I.**, Subsets of myeloid-derived suppressor cells in tumor-bearing mice. *J. Immunol.* 2008. **181**: 5791–5802.

36 **Sinha, P., Clements, V. K., Bunt, S. K., Albelda, S. M. and Ostrand-Rosenberg, S.**, Cross-talk between myeloid-derived suppressor cells and macrophages subverts tumor immunity toward a type 2 response. *J. Immunol.* 2007. **179**: 977–983.

37 **Cuervo, H., Pineda, M. A., Aoki, M. P., Gea, S., Fresno, M. and Girones, N.**, Inducible nitric oxide synthase and arginase expression in heart tissue during acute *Trypanosoma cruzi* infection in mice: arginase I is expressed in infiltrating CD68 +macrophages. *J. Infect. Dis.* 2008. **197**: 1772–1782.

38 **Nefedova, Y., Huang, M., Kusmartsev, S., Bhattacharya, R., Cheng, P., Salup, R., Jove, R. et al.**, Hyperactivation of STAT3 is involved in abnormal differentiation of dendritic cells in cancer. *J. Immunol.* 2004. **172**: 464–474.

39 **Nefedova, Y., Nagaraj, S., Rosenbauer, A., Muro-Cacho, C., Sebti, S. M. and Gabrilovich, D. I.**, Regulation of dendritic cell differentiation and antitumor immune response in cancer by pharmacologic-selective inhibition of the janus-activated kinase 2/signal transducers and activators of transcription 3 pathway. *Cancer Res.* 2005. **65**: 9525–9535.

40 **Poschke, I., Mougiakakos, D., Hansson, J., Masucci, G. V. and Kiessling, R.**, Immature immunosuppressive CD14+HLA-DR-/low cells in melanoma patients are Stat3hi and overexpress CD80, CD83, and DC-sign. *Cancer Res.* 2010. **70**: 4335–4345.

41 **Nagaraj, S., Gupta, K., Pisarev, V., Kinarsky, L., Sherman, S., Kang, L., Herber, D. L. et al.**, Altered recognition of antigen is a mechanism of CD8+ T cell tolerance in cancer. *Nat. Med.* 2007. **13**: 828–835.

42 **Wu, C. T., Hsieh, C. C., Lin, C. C., Chen, W. C., Hong, J. H. and Chen, M. F.**, Significance of IL-6 in the transition of hormone-resistant prostate cancer and the induction of myeloid-derived suppressor cells. *J. Mol. Med.* 2012. **90**: 1343–1355.

43 **Lopes, M. F. and DosReis, G. A.**, *Trypanosoma cruzi* induced immunosuppression: selective triggering of CD4+ T-cell death by the T-cell receptor-CD3 pathway and not by the CD69 or Ly-6 activation pathway. *Infect. Immun.* 1996. **64**: 1559–1564.

44 **Romani, L., Fallarino, F., De Luca, A., Montagnoli, C., D'Angelo, C., Zelante, T., Vacca, C. et al.**, Defective tryptophan catabolism underlies inflammation in mouse chronic granulomatous disease. *Nature* 2008. **451**: 211–215.

45 **Srivastava, M. K., Dubinett, S. and Sharma, S.**, Targeting MDSCs enhance therapeutic vaccination responses against lung cancer. *Oncoimmunology* 2012. **1**: 1650–1651.

46 **Cuenca, A. G., Delano, M. J., Kelly-Scumpia, K. M., Moreno, L. L., Scumpia, P. O., Laface, D. M., Heyworth, P. G. et al.**, A paradoxical role for myeloid-derived suppressor cells in sepsis and trauma. *Mol. Med.* 2011. **17**: 281–292.

47 **Jiao, Z., Hua, S., Wang, W., Wang, H., Gao, J. and Wang, X.**, Increased circulating myeloid-derived suppressor cells correlated negatively with Th17 cells in patients with rheumatoid arthritis. *Scand. J. Rheumatol.* 2013. **42**: 85–90.

48 **Yi, H., Guo, C., Yu, X., Zuo, D. and Wang, X. Y.**, Mouse CD11b+Gr-1+ myeloid cells can promote Th17 cell differentiation and experimental autoimmune encephalomyelitis. *J. Immunol.* 2012. **189**: 4295–4304.

49 **Alter, G., Malenfant, J. M. and Altfeld, M.**, CD107a as a functional marker for the identification of natural killer cell activity. *J. Immunol. Methods* 2004. **294**: 15–22.

Abbreviations: **5FU**: 5-fluorouracil · **Con A**: concavalina A · **IHL**: intrahepatic leukocyte · **MDSC**: myeloid-derived suppressor cell · **NAC**: N-acetyl L-cystein

Full correspondence: Dr. Susana Gea, Centro de Investigación en Bioquímica Clínica e Inmunología, CIBICI-CONICET, Facultad de Ciencias Químicas, Universidad Nacional de Córdoba, Cordoba-5000, Argentina
Fax: +54-0351-4333048-int: 3151
e-mail: sgea@fcq.unc.edu.ar

Additional correspondence: Alfredo Raul Arocena, Bioquimica Clinica, Centro de Investigacion en Bioquimica Clinica e Inmunologia, CIBICI-CONICET, Facultad de Ciencias Quimicas, Universidad Nacional de Cordoba, Cordoba-5000, Argentina
e-mail: aarocena@fcq.unc.edu.ar

Received: 10/4/2013
Revised: 29/7/2013
Accepted: 21/10/2013
Accepted article online: 25/10/2013

